DALTON

Crystal structure determination and *ab initio* molecular structure prediction for *exo,exo*-α-$P_4Se_3(CN)_2$, the first phosphorus selenide cyanide

Bruce W. Tattershall,* Emma L. Sandham and William Clegg

Department of Chemistry, University of Newcastle, Newcastle upon Tyne NE1 7RU, UK

Bicyclic *exo,exo*-α-$P_4Se_3(CN)_2$ **1** was made by reaction of α-$P_4Se_3I_2$ with AgCN, and its crystal structure determined from X-ray data collected at 160 K. Molecular structures were predicted for *exo,exo*-α-$P_4Se_3(CN)_2$, *exo,exo*-α-$P_4S_3(CN)_2$ and P_2Se_5 **2** by restricted Hartree–Fock *ab initio* molecular-orbital calculations using STO-3G, 3-21G* and LanL2DZ(d) ECP basis sets, and for P_2Se_5 additionally using Ahlrichs' split-valence and triple-zeta valence basis sets. Comparisons with the crystal structure of *exo,exo*-α-$P_4Se_3(CN)_2$ and with a previously published crystal structure of P_2Se_5 showed that the 3-21G* basis sets gave sufficiently good predictions for most bond angles that the effects on them of intermolecular interactions in the crystals could be discussed.

Molecules *exo,exo*-α-$P_4E_3R^1R^2$, where E = S or Se and R^1 and R^2 = H, halide or carbon-, nitrogen-, phosphorus- or sulfur-centred substituents, have been studied in solution by ^{31}P NMR spectroscopy.[1–6] This can provide detailed information about molecular structure, particularly about bond angles, but only when relationships between coupling constants or chemical shifts and geometric parameters have been established empirically. Until now, the only compounds in the series which have yielded crystals suitable for structure determination have been the iodides α-$P_4S_3I_2$ and α-$P_4Se_3I_2$.[7,8] To obtain structural data for correlation with NMR results we have therefore begun to predict molecular geometries by *ab initio* molecular orbital (MO) methods, using the program GAUSSIAN 94.[9] Semi-empirical or molecular modelling methods are not possible because of lack of parametrisation for molecules with polycyclic phosphorus chalcogenide skeletons.

Most reported *ab initio* work involving phosphorus has been aimed at testing the efficiency of increasingly sophisticated basis sets. Thus, Ahlrichs and co-workers[10,11] have optimised an improved split-valence (SV) basis {(10s,7p)/[4s,3p] for P or S; (14s,10p,5d)/[5s,4p,2d] for Se}[10] and a basis of valence triple-zeta (TZV) quality {(14s,9p)/[5s,4p] for P or S; (17s,13p,6d)/[6s,5p,2d] for Se}.[11] (In this notation the number of Gaussian-type primitive functions is in parentheses, and the number of functions into which they are contracted is in square brackets. To calculate the number of orbitals, the number of p functions should be multiplied by three and that of d functions by five.) These bases were tested using only very simple molecules, though the SVP set for phosphorus (SV augmented by one set of d polarisation functions) was recently used extensively for calculations on polyphosphane rings.[12] In previous work on selenium and other third-row atoms Binning and Curtiss calculated split-valence bases (14s,11p,5d)/[6s,4p,1d] and tested them in predicting several measured properties of simple molecules.[13] They concluded that simpler 3-21G* bases yielded molecular geometries which, in terms of differences from experimental geometries, were of similar quality {3-21G is a (12s,9p,3d)/[5s,4p,1d] contraction for Se, with corresponding s and p exponents constrained to be equal}. In calculations of NMR chemical shifts using the gauge-including atomic orbital method, less contracted basis sets have been used: (12s,9p)/[6s,5p] for phosphorus[14] and (14s,11p,5d)/[9s,6p,2d] for selenium.[15] In both cases, polarisation functions were added, and, for selenium, diffuse functions were also needed to account for the lone pairs of electrons.

For chemical shift calculations at least single-point all-electron calculations are required, since much of the nuclear shielding is by core electrons, but for calculations of geometry effective core potential (ECP) methods can in principle be used. Here, model potentials are substituted for core electrons, so that the number of basis functions is reduced. This offers little advantage for the second-row elements since time saved at the self-consistent field (SCF) stage is compensated by extra time spent at the gradient calculation stage, of each geometry optimisation cycle. In test calculations of the geometry of P_4S_3, constrained to C_{3v} symmetry, we found the following comparative times for one cycle of geometry optimisation: STO-3G, 88 s; 3-21G*, 317 s; Ahlrichs' SVP, 430 s; LanL2DZ(d) (a double-zeta ECP basis with one added d polarisation function),[16] 691 s. In contrast, for molecules containing many selenium atoms, the LanL2DZ(d) basis allows remarkably faster geometry optimisation even than 3-21G* (see below).

In contrast to most of the above work, we wished to make calculations on many molecules, each containing at least seven second-row atoms, as well as more or less complex exocyclic substituents centred on first-row atoms. In order to do this as an adjunct to preparative and NMR spectroscopic research, within modest use of supercomputer time and of man-hours spent in servicing the computations, we decided to resort to simpler basis sets than those developed recently. This should be possible as our aim was not to calculate accurate absolute energies or values of geometric or NMR parameters, but rather to calculate comparisons between similar molecules, or even between similar sites within a molecule. In such cases, systematic errors caused by use of small basis sets may be expected to cancel out to some extent. We found at an early stage that the minimal basis set STO-3G is of little use, since it gives qualitatively unrealistic geometries for nitrogen-centred substituents bonded to phosphorus.[17] (For the molecules reported here, where substantial π bonding to phosphorus is not expected, STO-3G calculations were a useful intermediate stage, and are reported.) Since most of our work involved molecules with phosphorus sulfide skeletons, we opted to use 3-21G* basis sets in restricted Hartree–Fock (RHF) calculations as a probable best compromise, and have calculated geometries which have been useful in rationalising trends in NMR parameters in several cases.[17,18] However, a comparison of a predicted molecular structure with a measured structure is desirable, to verify that the results are reasonably realistic.

We now report the synthesis of the first phosphorus selenide cyanide, *exo,exo*-α-$P_4Se_3(CN)_2$ **1** (E = Se), which yielded well formed crystals, enabling an X-ray diffraction analysis.

Table 1 Phosphorus-31 NMR data[a] for *exo,exo*-α-$P_4E_3(CN)_2$ (E = Se or S)

	E = Se	E = S[b]
$\delta(P_A)$	106.16	128.69
$\delta(P_B)$	29.17	34.18
$^2J(P_AP_C)$	95.73(7)	86.3
$^1J(P_AP_B)$	−252.11(5)	−254.7
$^2J(P_AP_D)$	34.63(3)	32.1
$^3J(P_BP_D)$	−19.26(4)	−14.4

[a] Solvent: CS_2. Chemical shifts are in ppm relative to H_3PO_4–water and coupling constants are in Hz with standard deviations (σ) in parentheses. Atom labelling is shown in Scheme 1. [b] Ref. 1.

Although the molecule presented its own difficulties in *ab initio* structure prediction, this has now been accomplished. Use of a 3-21G* basis set gives a geometry which is very similar to that found in the crystal. We also report, for comparison, predictions of molecular geometry for *exo,exo*-α-$P_4S_3(CN)_2$.

While the bicyclic molecule P_2Se_5 **2** is an isolated case offering no sites for exocyclic substitution and hence empirical correlations, its crystal structure has been reported.[19] Its molecular geometry is sufficiently similar to that of the skeleton of *exo,exo*-α-$P_4Se_3(CN)_2$ for useful comparisons to be made. We have therefore further tested use of the 3-21G* basis set for selenium compounds by predicting the structure of P_2Se_5. We verified that much better agreement with the crystal structure geometry was not produced by more expensive calculations using Ahlrichs' SVP or TZVP+ basis sets. The LanL2DZ(d) ECP method gave similar results to the 3-21G* basis for all three molecules.

Results and discussion

Synthesis of *exo,exo*-α-$P_4Se_3(CN)_2$

The analogous compound *exo,exo*-α-$P_4S_3(CN)_2$ was first made by Fluck *et al.*[20] by stirring a solution of α-$P_4S_3I_2$ in CS_2 with solid AgCN over 5 d at 50 °C. This silver salt method of making compounds α-$P_4E_3X_2$ offers the possibility of yielding a pure solution of the product, since the AgI formed is extremely insoluble. The sulfide cyanide was always accompanied, however, by substantial impurities,[1] a minor one of which was later identified as the invertomer *endo,exo*-α-$P_4S_3(CN)_2$,[6] and crystals suitable for structure determination could not be obtained.

In contrast to this, α-$P_4Se_3I_2$ reacted completely with an excess of AgCN at room temperature (20 °C) in 5 d, to give a solution containing only *exo,exo*-α-P_4Se_3(I)CN, *exo,exo*-α-$P_4Se_3(CN)_2$ **1**, and *endo,exo*-α-$P_4Se_3(CN)_2$, in molar ratio 48:29:23. Further stirring of the mixture at 52 °C for 1 d then caused the complete further reaction of *exo,exo*-α-P_4Se_3(I)CN and disappearance of all but a trace of *endo,exo*-α-$P_4Se_3(CN)_2$, to leave *exo,exo*-α-$P_4Se_3(CN)_2$ as the only phosphorus-containing solute in significant concentration. The solution was saturated without further concentration, and a sample taken at 42 °C gave well formed yellow crystals on slow cooling to 20 °C. A full NMR study including all three products will be reported separately as part of a larger work:[21] only the chemical shifts and coupling constants from the main ^{31}P NMR spectrum of *exo,exo*-α-$P_4Se_3(CN)_2$ are included here for identification purposes. Table 1 shows that these compare well with corresponding parameters for *exo,exo*-α-$P_4S_3(CN)_2$. The lower value of $\delta(P_A)$ in the selenium compound may be attributed to the effect of the lower electronegativity of two neighbouring selenium atoms.

Crystal structure

The asymmetric unit consists of a single complete molecule, which thus has no crystallographic symmetry. The essential

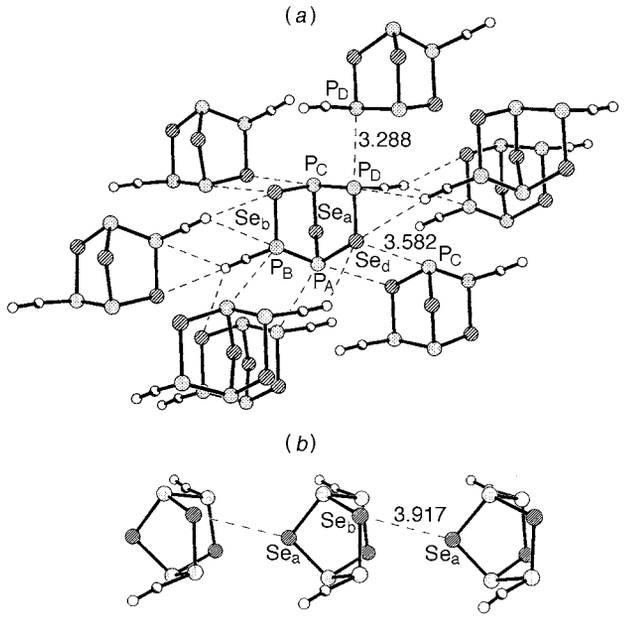

Fig. 1 Crystal packing of *exo,exo*-α-$P_4Se_3(CN)_2$ **1**, showing interactions (*a*) between stacks and (*b*) along a stack. Distances in Å

symmetry of the molecule, but not of its crystalline environment, is C_2. The complete molecular geometry is given in Table 2 and views of it in Fig. 1.

Ab initio molecular structure prediction

A molecular geometry for *exo,exo*-α-$P_4Se_3(CN)_2$ with C_2 symmetry was derived from the observed non-symmetric geometry in the crystal, by averaging corresponding pairs of bond lengths or angles required for a *Z* matrix. Starting from this, *ab initio* geometry optimisation was performed with C_2 symmetry imposed, first at the RHF/STO-3G, then at the RHF/3-21G* level. A major difficulty resulted from the near-linearity of the P–C–N chains. The average bond angle at carbon in the crystal was 173.6° and was predicted in the free molecule to be 177.12 (STO-3G) or 177.36° (3-21G*). This resulted in a rather flat energy minimum with respect to rotation about the P–C bond. The geometry of the P_4Se_3 skeleton varied little once it had approached the optimum, but it depended sufficiently on the orientation of the CN group to make us reluctant to fix arbitrarily the rotational position. The convergence tests built in to GAUSSIAN 94 were eventually satisfied only when the newly available redundant internal coordinates method, rather than *Z*-matrix variable optimisation, was used, and then only after 29 optimisation cycles at the STO-3G level and 18 at the 3-21G* level. Similar difficulties were encountered in corresponding calculations for *exo,exo*-α-$P_4S_3(CN)_2$. For both molecules, the calculations were confirmed by reoptimisation using the Los Alamos LanL2DZ(d) ECP basis sets. Relative times for one (final) cycle of geometry optimisation using the STO-3G, 3-21G* and ECP bases were 317, 1942 and 2315 s for *exo,exo*-α-$P_4Se_3(CN)_2$, or 94 (*Z*-matrix method), 899 and 1989 s for *exo,exo*-α-$P_4S_3(CN)_2$.

Using the redundant internal coordinate method for P_2Se_5, only 31 geometric parameters are optimised (of which five are independent under C_{2v} symmetry), compared with 51 for *exo,exo*-α-$P_4Se_3(CN)_2$. This, together with the absence of difficulties caused by exocyclic substituents, made P_2Se_5 a suitable molecule for which to study the use of more sophisticated basis sets. Geometry optimisation was carried out using Ahlrichs' SVP or TZVP+ bases, or the LanL2DZ(d) ECP basis (see Table 2 footnotes), in addition to using the STO-3G or 3-21G* bases. Relative times for one cycle of geometry optimisation, with symmetry constrained to C_{2v}, were 248, 1190, 2700, 5192 and 575 s, for the STO-3G, 3-21G*, SVP, TZVP+ and ECP basis

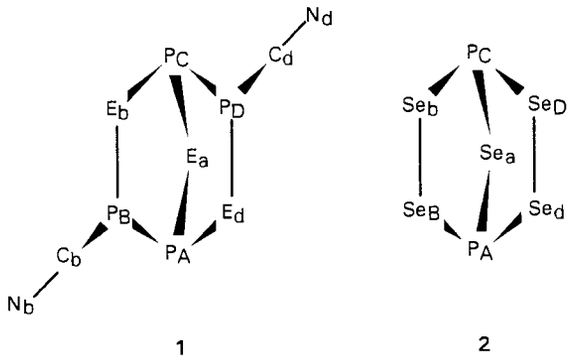

Scheme 1 Labelling of atoms for *exo,exo*-α-$P_4E_3(CN)_2$ **1** (E = S or Se) and P_2Se_5 **2**

sets. Prediction of the geometry of P_2Se_5 raised the question of whether the free molecule necessarily has C_{2v} symmetry. It seemed possible that the six-membered ring might adopt a twist-boat rather than a simple boat configuration, depending on what distance $P_A \cdots P_C$ (Scheme 1)† was best stabilised by the Se_a bridge. This would result in the selenium atoms of the six-membered ring forming two pairs related by C_2 symmetry. The non-equivalent atoms within each pair would differ only in long-range interactions within the molecule; *e.g.* the distances $Se_a \cdots Se_b$ and $Se_a \cdots Se_B$ would be different. There would therefore be a low-energy path for deformation through the boat form with C_{2v} symmetry to the enantiomer twisted in the opposite sense, and it would not be surprising that all selenium atoms in the six-membered ring appear chemically equivalent on the NMR time-scale,[22] even at 240 K.[23] To investigate this, we constrained the *ab initio* optimisations of geometry for P_2Se_5 only to C_2 rather than to C_{2v} symmetry in calculations using the STO-3G, 3-21G* or ECP bases, but Table 2 shows that the twist angle P_A–Se_B–Se_b–P_C is predicted to be zero, probably to within the accuracy of these methods. The C_{2v} symmetry is thus confirmed. The twist angles found in the crystal structure were much larger and of opposite sign,[19] corresponding to a deformation giving a substantial difference in 'book angles' Se_B–P_A–Se_d and Se_b–P_C–Se_D (108.44 and 104.88°). This seems very unlikely in the free molecule and was not tested in the present calculations. In the crystal structure it is readily attributable to intermolecular Se ··· Se and P ··· Se interactions, discussed below.

Comparison of measured and predicted structures

Bond lengths and angles and a selection of torsion angles predicted by *ab initio* calculation for *exo,exo*-α-$P_4Se_3(CN)_2$, *exo,exo*-α-$P_4S_3(CN)_2$ and P_2Se_5 are compared in Table 2 with values from the crystal structures of *exo,exo*-α-$P_4Se_3(CN)_2$ and P_2Se_5.

For P_2Se_5 the root mean square (r.m.s.) deviation between predicted and measured bond angles was 1.68, 1.11, 0.97, 0.92 and 0.98°, using the STO-3G, 3-21G*, SVP, TZVP+ and ECP basis sets respectively. There was some balancing of deviations in bond angles. If angles in the crystal structure which would be equal under C_{2v} symmetry were averaged, then the r.m.s. deviations from the *ab initio* predictions, of these averaged values, had lower values for the five basis sets: 1.44, 0.70, 0.47, 0.35 and 0.49°. Corresponding r.m.s. deviations for bond lengths from individual crystal values were 0.020, 0.019, 0.014, 0.015 and 0.018 Å compared with σ values of about 0.002 Å for the crystal structure data. As anticipated by the designers of the SVP basis set,[10] there is little useful extra accuracy of geometrical parameters to be gained, in RHF calculations, by spending

† For purposes of comparison, for α-$P_4E_3(CN)_2$ **1**, similar atom labelling has been used throughout this paper as in previous NMR-based papers (*e.g.* ref. 5); P_2Se_5 **2** has been labelled to correspond to this.

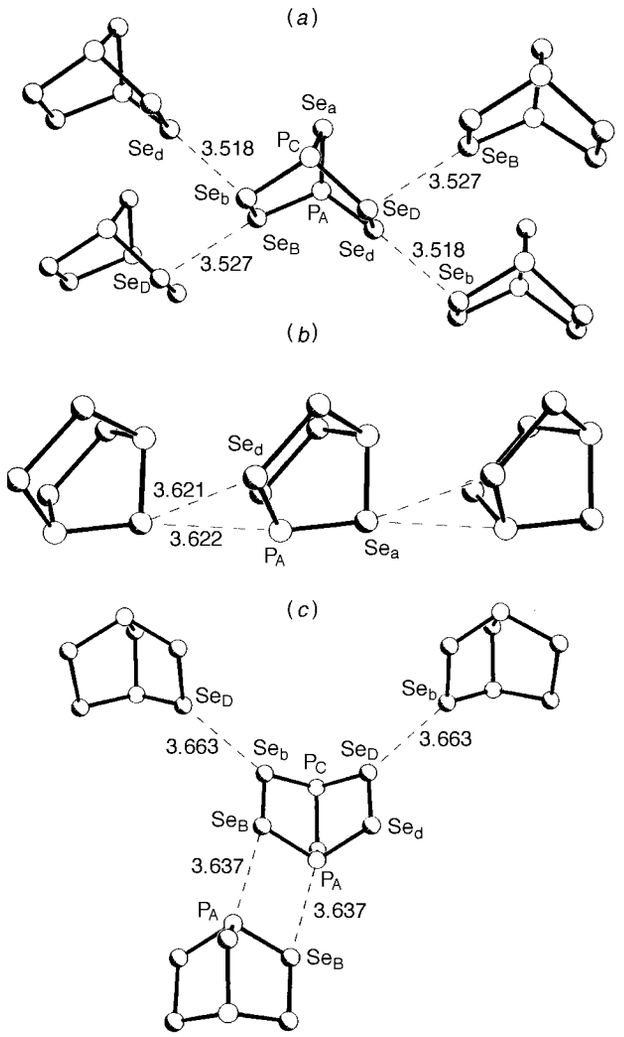

Fig. 2 Crystal packing of P_2Se_5 **2** (from atomic coordinates in ref. 19), showing interactions (*a*) between chains (*b*) along a chain and (*c*) between layers. Distances in Å

nearly twice as much computer time in going from the SVP to the TZVP+ basis. If the TZVP+ geometry is assumed to be 'correct' for the free molecule, then, while bond lengths and non-bonded lengths are generally too short from 3-21G* calculations, bond angles, which are the most useful parameters on which to base qualitative discussion of observed NMR results, are predicted accurately enough at the 3-21G* level. At less than half the computer-time requirements of the SVP basis, our choice of the 3-21G* level for the rest of the calculations is thus justified. None of the arguments below about the effect of crystal interactions, based on the 3-21G* geometry, needed to be changed to agree with the result of the TZVP+ calculation. The STO-3G model was not sufficiently accurate to be used as a basis for these arguments. In the particular case of a compound with several selenium atoms and relatively few internal geometric coordinates, the ECP method is clearly to be preferred over any of the others.

Most of the larger deviations from predictions at the 3-21G* level for P_2Se_5 can be explained in terms of intermolecular interactions in the crystal. Thus, intermolecular Se ··· Se interactions, at 3.53 and 3.52 Å, act on Se_B and Se_d respectively approximately collinearly with their intramolecular bonds to P_A, so as to have little effect on bond angles, but on Se_D and Se_b approximately normally to their bonds to P_C [Fig. 2(*a*)]. This causes a decrease in book angle Se_D–P_C–Se_b to less than its value in the free molecule. Another set of intermolecular interactions exists between Se_a in one molecule and P_A and Se_d (both at 3.62 Å) in the next, to form chains nearly collinear with the intra-

Table 2 Geometric parameters for *exo,exo*-α-$P_4E_3(CN)_2$ (E = Se or S) and P_2Se_5

	exo,exo-α-$P_4Se_3(CN)_2$				*exo,exo*-α-$P_4S_3(CN)_2$				P_2Se_5					
Method:	Crystal[a]	STO-3G	3-21G*	ECP[b]	STO-3G	3-21G*	ECP[b]		Crystal[a,c]	STO-3G	3-21G*	SVP[d]	TZVP+[e]	ECP[b]
Symmetry constraint:	None	C_2	C_2	C_2	C_2	C_2	C_2		None	C_2	C_2	C_{2v}	C_{2v}	C_2
(*a*) Bond lengths (Å)														
$P_C–E_a$	2.241(2)	2.251	2.229	2.259	2.102	2.098	2.113	$P_C–Se_a$	2.246(2)	2.256	2.234	2.262	2.262	2.265
$P_C–P_D$	2.205(2)	2.210	2.199	2.227	2.206	2.211	2.234	$P_C–Se_D$	2.251(2)	2.270	2.228	2.257	2.261	2.261
$P_C–E_b$	2.268(2)	2.269	2.254	2.282	2.118	2.125	2.140	$P_C–Se_b$	2.254(2)	2.270	2.228	2.257	2.261	2.261
$P_A–E_a$	2.241(2)	2.251	2.229	2.259	2.102	2.098	2.113	$P_A–Se_a$	2.233(2)	2.256	2.234	2.262	2.262	2.265
$P_A–P_B$	2.201(2)	2.210	2.199	2.227	2.206	2.211	2.234	$P_A–Se_B$	2.244(2)	2.270	2.228	2.257	2.261	2.261
$P_A–E_d$	2.267(2)	2.269	2.254	2.282	2.118	2.125	2.140	$P_A–Se_d$	2.245(2)	2.270	2.228	2.257	2.261	2.261
$P_B–E_b$	2.272(2)	2.279	2.263	2.299	2.130	2.131	2.146	$Se_B–Se_b$	2.387(1)	2.371	2.365	2.398	2.393	2.405
$P_B–C_b$	1.799(6)	1.786	1.778	1.790	1.788	1.777	1.791							
$P_D–E_d$	2.263(2)	2.279	2.263	2.299	2.130	2.131	2.146	$Se_D–Se_d$	2.390(1)	2.371	2.365	2.398	2.393	2.405
$P_D–C_d$	1.786(6)	1.786	1.778	1.790	1.788	1.777	1.791							
$C_b–N_b$	1.145(8)	1.157	1.142	1.155	1.156	1.142	1.155							
$C_d–N_d$	1.148(8)	1.157	1.142	1.155	1.156	1.142	1.155							
(*b*) Bond angles (°)														
$P_C–E_a–P_A$	98.14(6)	98.63	97.13	97.13	100.24	100.02	100.12	$P_C–Se_a–P_A$	97.65(8)	99.06	96.14	96.53	96.68	96.48
$E_a–P_C–P_D$	102.29(7)	101.45	101.71	102.46	99.98	100.34	100.44	$Se_a–P_C–Se_D$	101.31(9)	101.13	102.40	102.11	101.91	102.13
$E_a–P_C–E_b$	103.64(6)	101.64	104.58	103.47	102.00	102.90	102.69	$Se_a–P_C–Se_b$	102.00(7)	101.11	102.40	102.11	101.91	102.13
$P_D–P_C–E_b$	93.25(7)	98.11	95.98	97.41	98.54	96.77	97.00	$Se_D–P_C–Se_b$	104.88(9)	103.77	106.17	106.48	106.63	106.69
$E_a–P_A–P_B$	102.97(7)	101.45	101.71	102.46	99.98	100.34	100.44	$Se_a–P_A–Se_B$	102.20(9)	101.13	102.40	102.11	101.91	102.13
$E_a–P_A–E_d$	103.99(6)	101.64	104.58	103.47	102.00	102.90	102.69	$Se_a–P_A–Se_d$	100.90(7)	101.11	102.40	102.11	101.91	102.13
$P_B–P_A–E_d$	93.27(7)	98.11	95.98	97.41	98.54	96.77	97.00	$Se_B–P_A–Se_d$	108.44(9)	103.77	106.17	106.48	106.63	106.69
$P_A–P_B–E_b$	105.18(7)	104.16	104.72	104.37	103.28	102.23	102.30	$P_A–Se_B–Se_b$	102.13(5)	103.53	102.42	102.51	102.62	102.44
$P_A–P_B–C_b$	96.4(2)	96.55	97.16	97.14	96.30	96.65	96.77							
$E_b–P_B–C_b$	99.3(2)	99.21	100.39	100.45	98.90	100.44	100.48							
$P_A–E_d–P_D$	103.02(5)	104.93	102.80	103.37	106.03	106.45	106.53	$P_A–Se_d–Se_D$	102.37(6)	103.52	102.42	102.51	102.62	102.44
$P_C–P_D–E_d$	105.92(7)	104.16	104.72	104.37	103.28	102.23	102.30	$P_C–Se_D–Se_d$	102.80(6)	103.53	102.42	102.51	102.62	102.44
$P_C–P_D–C_d$	96.0(2)	96.55	97.16	97.14	96.30	96.65	96.77							
$E_d–P_D–C_d$	100.2(2)	99.21	100.39	100.45	98.90	100.44	100.48							
$P_C–E_b–P_B$	103.57(5)	104.93	102.80	103.37	106.03	106.45	106.53	$P_C–Se_b–Se_B$	103.12(6)	103.52	102.42	102.51	102.62	102.44
$P_B–C_b–N_b$	173.7(6)	177.12	177.36	176.00	177.53	177.09	176.17							
$P_D–C_d–N_d$	173.5(6)	177.12	177.36	176.00	177.53	177.09	176.17							

Table 2 (*continued*)

	exo,exo-α-$P_4Se_3(CN)_2$				*exo,exo*-α-$P_4S_3(CN)_2$				P_2Se_5					
Method:	Crystal [a]	STO-3G	3-21G*	ECP [b]	STO-3G	3-21G*	ECP [b]		Crystal [a,c]	STO-3G	3-21G*	SVP [d]	TZVP+ [e]	ECP [b]
Symmetry constraint:	None	C_2	C_2	C_2	C_2	C_2	C_2		None	C_2	C_2	C_{2v}	C_{2v}	C_2
(*c*) Selected torsion angles (°) [f]														
$P_A–E_a–P_C–P_D$	49.88(7)	52.98	52.67	52.36	51.05	51.80	51.36	$P_A–Se_a–P_C–Se_D$	54.85	53.27	54.95	55.02	55.05	55.14
$P_A–E_a–P_C–E_b$	−46.59(6)	−47.90	−46.76	−48.51	−50.00	−47.68	−48.34	$P_A–Se_a–P_C–Se_b$	−53.22	−53.34	−54.95	−55.02	−55.05	−55.14
$P_C–E_a–P_A–P_B$	49.99(7)	52.98	52.67	52.36	51.05	51.80	51.36	$P_C–Se_a–P_A–Se_B$	55.13	53.27	54.95	55.02	55.05	55.14
$P_C–E_a–P_A–E_d$	−46.77(6)	−47.90	−46.76	−48.51	−50.00	−47.68	−48.34	$P_C–Se_a–P_A–Se_d$	−56.66	−53.34	−54.95	−55.02	−55.05	−55.14
$E_a–P_C–P_D–C_d$	67.65(19)	64.43	63.35	66.34	67.62	65.89	67.31							
$P_D–P_C–E_b–P_B$	−77.16(7)	−77.73	−80.30	−77.66	−73.83	−78.04	−76.73	$Se_D–P_C–Se_b–Se_B$	−74.07	−72.06	−72.95	−72.72	−72.51	−72.75
$E_a–P_A–P_B–C_b$	67.04(20)	64.43	63.35	66.34	67.62	65.89	67.31							
$P_B–P_A–E_d–P_D$	−78.15(7)	−77.73	−80.30	−77.66	−73.83	−78.04	−76.73	$Se_B–P_A–Se_d–Se_D$	−70.86	−72.06	−72.95	−72.72	−72.51	−72.75
$P_A–P_B–E_b–P_C$	4.92(8)	6.74	9.74	5.64	3.01	7.44	5.76	$P_A–Se_B–Se_b–P_C$	2.18	−0.10	0.00	0.00	0.00	0.00
$P_A–P_B–C_b–N_b$	125(5)	129.03	128.51	125.95	132.68	133.13	130.22							
$E_b–P_B–C_b–N_b$	−128(5)	−125.42	−125.03	−127.93	−122.77	−123.08	−125.89							
$P_A–E_d–P_D–P_C$	5.37(8)	6.74	9.74	5.64	3.01	7.44	5.76	$P_A–Se_d–Se_D–P_C$	−2.53	−0.10	0.00	0.00	0.00	0.00
$P_C–P_D–C_d–N_d$	110(5)	129.03	128.51	125.95	132.68	133.13	130.22							
$E_d–P_D–C_d–N_d$	−143(5)	−125.42	−125.03	−127.93	−122.77	−123.08	−125.89							
(*d*) Selected intramolecular non-bonded distances (Å)														
$P_A \cdots P_C$	3.387(2)	3.414	3.342	3.387	3.226	3.215	3.241	$P_A \cdots P_C$	3.371	3.433	3.323	3.375	3.380	3.379
$P_A \cdots P_D$	3.546(2)	3.606	3.531	3.594	3.394	3.409	3.435	$P_A \cdots Se_D$	3.613	3.645	3.581	3.631	3.633	3.639
$P_B \cdots P_C$	3.567(2)	3.606	3.531	3.594	3.394	3.409	3.435	$Se_B \cdots P_C$	3.636	3.645	3.581	3.631	3.633	3.639
$P_B \cdots P_D$	4.016(3)	4.198	4.115	4.169	3.959	4.009	4.024	$Se_B \cdots Se_D$	4.329	4.285	4.276	4.339	4.344	4.353
$P_B \cdots E_a$	3.476(2)	3.453	3.434	3.498	3.301	3.310	3.342	$Se_B \cdots Se_a$	3.484	3.496	3.477	3.514	3.513	3.521
$P_B \cdots E_d$	3.248(2)	3.383	3.309	3.388	3.278	3.243	3.277	$Se_B \cdots Se_d$	3.642	3.572	3.562	3.616	3.626	3.628
$P_D \cdots E_a$	3.463(2)	3.453	3.434	3.498	3.301	3.310	3.342	$Se_D \cdots Se_a$	3.477	3.496	3.477	3.514	3.513	3.521
$P_D \cdots E_b$	3.252(2)	3.383	3.309	3.388	3.278	3.243	3.277	$Se_D \cdots Se_b$	3.571	3.572	3.562	3.616	3.626	3.628
$E_a \cdots E_b$	3.544(1)	3.504	3.547	3.565	3.280	3.303	3.321	$Se_a \cdots Se_b$	3.497	3.495	3.477	3.514	3.513	3.521
$E_a \cdots E_d$	3.552(1)	3.504	3.547	3.565	3.280	3.303	3.321	$Se_a \cdots Se_d$	3.453	3.495	3.477	3.514	3.513	3.521
$E_b \cdots E_d$	3.900(1)	3.945	3.874	4.008	3.859	3.743	3.805	$Se_b \cdots Se_d$	4.322	4.289	4.276	4.339	4.344	4.353

[a] Standard deviations (σ) in parentheses. [b] Los Alamos LanL2DZ ECP basis (ref. 16) augmented by one d polarisation function of P, S or Se (exponents 0.45, 0.55, 0.338). [c] From atomic coordinates in ref. 19. [d] Ahlrichs' split-valence polarisation basis (ref. 10). [e] Ahlrichs' triple-zeta valence basis (ref. 11) augmented by one d polarisation function (same exponents, P 0.45, Se 0.338, as for SVP) and one sp-type diffuse function (exponents P 0.0348, Se 0.0220). [f] Torsion angle A–B–C–D is the angle between projections of vectors BA and CD on a plane perpendicular to BC.

molecular Se_a–P_A bonds [Fig. 2(*b*)]. This causes an opening of the intramolecular book angle Se_B–P_A–Se_d to greater than the free-molecule value, to make room for the distant selenium to interact with P_A, while the five-membered ring angle Se_a–P_A–Se_d is compressed. The other partner in this interaction, Se_a, is displaced intramolecularly in the direction of P_A, increasing the bond angle at Se_a. Longer intermolecular interactions (at 3.64 and 3.66 Å) exist between layers [Fig. 2(*c*)]. If the interaction $Se_D \cdots Se_b$ is repulsive, but $P_A \cdots Se_B$ is attractive, an increase in bond angle at Se_b and a decrease in that at Se_B is explained.

The larger molecule *exo,exo*-α-$P_4Se_3(CN)_2$ is affected by a much more complex network of intermolecular interactions in the crystal. The r.m.s. deviations between predicted and crystal geometry were 2.4, 1.8 and 1.8° for bond angles, and 0.009, 0.010 and 0.019 Å for bond lengths, at the STO-3G, 3-21G* and ECP levels. As for P_2Se_5, bond lengths predicted using the ECP basis were too long, and for *exo,exo*-α-$P_4Se_3(CN)_2$ those predicted using the 3-21G* basis were nearer to those measured in the crystal. The ECP and 3-21G* bases gave predictions of similar accuracy, as judged by comparison with crystal data, of some bond angles, but for others the geometry in the crystal is clearly strongly perturbed, compared with either prediction for the free molecule. The following discussion will be based on the 3-21G* predictions. In contrast to the P_2Se_5 case, molecules stack with their approximate C_2 axes aligned with the *b* crystallographic axis [Fig. 1(*b*)]: the shortest interaction along the stack, between Se_a and Se_b in the next molecule, is long (3.92 Å) and the stack seems to be held together mainly by stronger interactions with molecules in both directions along neighbouring stacks [Fig. 1(*a*)]. Several of these involve nitrogen or P_B (or P_D), which are predicted at the RHF/3-21G* level to carry significant charges (−0.41 and +0.51 respectively). While the environments of P_B, P_A and Se_d are different from those of P_D, P_C and Se_b [Fig. 1(*a*)], the effect of intermolecular interactions, in contrast to the P_2Se_5 case, is to close both book angles P_D–P_C-Se_b and P_B–P_A–Se_d, rather than to close one and open the other. The contact between Se_d and a distant P_C (at 3.58 Å) is the shortest of the clearly book-closing interactions. Distant nitrogen atoms interact with Se_b, P_B, Se_d and P_D at 3.38, 3.31, 3.31 and 3.18 Å, but are almost in the approximate planes of the P_A–P_B–Se_b–P_C or P_C–P_D–Se_d–P_A half rings. Instead of closing the book angles, these interactions may be responsible for compressing the half rings so as to open the six-membered ring angles at Se_b, P_B and P_D, with widening of the angle at Se_a. The opening of the ring angles is augmented for P_D and is rendered negligible for Se_d by a strong intermolecular interaction (3.29 Å) between atoms P_D on neighbouring enantiomeric molecules. This acts approximately along the line of the P_D–Se_d bond and has no counterpart on the P_B side of the molecule. Bond length P_D–Se_d is rendered shorter than P_B–Se_b. The shortness of the $P_D \cdots P_D$ contact may reflect a decrease in the van der Waals radius of P_D, associated with its positive charge. While interactions with N_d are nearly along the line of the P–C–N sequence, those with N_b have the effect of closing angle Se_b–P_B–C_b.

Comparison between predicted structures for *exo,exo*-α-$P_4Se_3(CN)_2$ and *exo,exo*-α-$P_4S_3(CN)_2$

Calculations using the 3-21G* and ECP bases gave almost identical skeletal bond angles to each other for *exo,exo*-α-$P_4S_3(CN)_2$. Changes in endocyclic bond angles in going from predicted values for *exo,exo*-α-$P_4S_3(CN)_2$ to those for *exo,exo*-α-$P_4Se_3(CN)_2$ are very similar to changes in the corresponding angles in going from the measured crystal structure of α-$P_4S_3I_2$ to that of α-$P_4Se_3I_2$.[7,8] The distance $S_a \cdots S_b$ or $S_a \cdots S_d$ in the sulfur compound is, at 3.303 Å (3-21G* results, Table 2), much shorter than the sum of the van der Waals radii (3.60 Å). Replacing sulfur by selenium forces an increase in separation of the chalcogen nuclei to 3.547 Å, compared with a radius sum of 3.80 Å. This can be accomplished only by decreases in bond angles at all three chalcogen atoms. The decreases are larger than on going from crystalline S_8 to crystalline Se_8, where comparable repulsions do not exist. Within the five-membered rings, the decreases are compensated by increases in bond angles at all three phosphorus atoms, including P_B (or P_D) even though non-bonded distances $P_B \cdots E_a$ (3.310 changing to 3.434 Å) and $P_B \cdots E_d$ (3.243 changing to 3.309 Å) are also within the van der Waals radius sums (3.65 changing to 3.75 Å). The sum of bond angles at the bridgehead atoms P_A or P_C increases by 2.26°. Opening of the book angles is probably resisted by lone-pair repulsion at the bridgehead atoms (valence shell electron pair repulsion effect), and possibly by an attractive interaction $P_B \cdots E_d$. As noted above, crystal forces appear capable of further reducing the book angles in the selenium compound, so as to return $P_B \cdots P_D$ to a value close to that for the sulfur compound.

Despite changes in endocyclic bond lengths and angles at P_B or P_D, the bond lengths and angles to carbon are practically unaffected by chalcogen substitution, as is the geometry of the cyanide group. This is in contrast to the crystal structures of the iodides, where replacement of sulfur by selenium results in an increase in bond angles to iodine. It probably shows that, in contrast to iodine, cyanide has little intramolecular nonbonded interaction with the molecular skeleton.

Experimental

Preparation of *exo,exo*-α-$P_4Se_3(CN)_2$ 1 (E = Se)

Silver cyanide was freshly prepared by addition of $AgNO_3$–water to KCN–water, with care that the final solution was not alkaline. It was washed with ethanol and dried by pumping at high vacuum for 3 h at 20 °C. All subsequent operations were carried out under nitrogen, using Schlenk methods. The compound α-$P_4Se_3I_2$ was made by reaction of stoichiometric quantities of red P, grey Se and I_2 in a sealed ampoule at 240–300 °C over 3 d, followed by Soxhlet extraction using CS_2.

Silver cyanide (1.071 g, 8.00 mmol) was added to crystalline α-$P_4Se_3I_2$ (0.615 g, 1.00 mmol) and the mixture stirred vigorously with CS_2 (20 cm^3) for 5 d at 20 °C, then at 52 °C for 24 h, with protection from light. During this second stage the solution changed from mid-yellow to almost colourless. The temperature was reduced to 42 °C for sampling of the supernatant liquid by pipette to a clean Schlenk tube. This was allowed to cool slowly in a large oil-bath to 20 °C, when crystals of *exo,exo*-α-$P_4Se_3(CN)_2$ **1** (E = Se) were obtained and removed by pipette. The NMR spectra of solutions were measured in 10 mm diameter tubes with a precision capillary containing $(CD_3)_2CO$ for locking, using a Bruker WM300WB spectrometer operating at 121.5 MHz for ^{31}P. Spectra were fitted using the program NUMARIT.[24]

X-Ray crystallography

Crystal data for *exo,exo*-α-$P_4Se_3(CN)_2$ 1 (E = Se). $C_2N_2P_4Se_3$, $M = 412.80$, monoclinic, space group $P2_1/c$, $a = 13.898(2)$, $b = 6.3903(11)$, $c = 11.882(2)$ Å, $\beta = 109.397(4)°$, $U = 995.4(3)$ $Å^3$, $Z = 4$, $D_c = 2.755$ g cm^{-3}, $\mu = 11.67$ mm^{-1} (Mo-Kα, $\lambda = 0.710\ 73$ Å), $F(000) = 752$, $T = 160$ K.

A yellow crystal of size 0.50 × 0.38 × 0.06 mm was examined on a Siemens SMART CCD area-detector diffractometer. Intensities were integrated from several series of frames covering 0.3° each in ω, the total data set corresponding to more than a hemisphere of reciprocal space. Remeasurement of the initial frames at the end of data collection indicated no significant change in intensity. Semiempirical absorption corrections were applied, based on repeated and symmetry-equivalent reflections in the data set (transmission 0.121–0.623). 3603 Measured

reflections yielded 1616 unique data with $R_{int} = 0.0853$ and $\theta_{max} = 25.31°$.

All atoms were located by direct methods and were refined with anisotropic displacement parameters by full-matrix least-squares methods based on F^2, with the weighting scheme $w^{-1} = \sigma^2(F_o^2) + (0.0567P)^2 + (1.6241P)$, where $P = (2F_c^2 + F_o^2)/3$. An isotropic extinction parameter x refined to 0.0025(5), whereby F_c is multiplied by $(1 + 0.001xF_c^2\lambda^3/\sin 2\theta)^{-1/4}$. At convergence, $R' = [\Sigma w(F_o^2 - F_c^2)^2/\Sigma w(F_o^2)^2]^{1/2} = 0.1097$ for all data, conventional $R = 0.0385$ on F values of 1459 reflections having $F_o^2 > 2\sigma(F_o^2)$, goodness of fit = 1.121 on F^2 for all data and 101 refined parameters. Extremes of the final difference map were +0.64 and −1.04 e Å^{-3}. Programs: Siemens SMART and SAINT control and integration software, SHELXTL.[25]

Atomic coordinates, thermal parameters, and bond lengths and angles have been deposited at the Cambridge Crystallographic Data Centre (CCDC). See Instructions for Authors, *J. Chem. Soc., Dalton Trans.*, 1996, Issue 1. Any request to the CCDC for this material should quote the full literature citation and the reference number 186/258.

Acknowledgements

We thank the EPSRC for provision of X-ray equipment (to W. C.) and for a grant of vector supercomputer resources (to B. W. T.) for *ab initio* calculations. Dr M. N. S. Hill is thanked for assistance in obtaining NMR spectra, and Dr M. R. J. Elsegood for assistance in analysis of the crystal packing.

References

1 B. W. Tattershall, *J. Chem. Soc., Dalton Trans.*, 1987, 1515.
2 B. W. Tattershall, *J. Chem. Soc., Dalton Trans.*, 1991, 483.
3 R. Blachnik, K. Hackmann and H.-P. Baldus, *Z. Naturforsch., Teil B*, 1991, **46**, 1165.
4 R. Blachnik and K. Hackmann, *Phosphorus Sulfur Silicon Relat. Elem.*, 1992, **65**, 99.
5 B. W. Tattershall and N. L. Kendall, *J. Chem. Soc., Dalton Trans.*, 1993, 3163.
6 B. W. Tattershall and N. L. Kendall, *Polyhedron*, 1994, **13**, 1507.
7 D. A. Wright and B. R. Penfold, *Acta Crystallogr.*, 1959, **12**, 455; B. W. Tattershall, N. L. Kendall, A. McCamley and W. Clegg, *Acta Crystallogr., Sect. C*, 1993, **49**, 571.
8 R. Blachnik, G. Kurz and U. Wickel, *Z. Naturforsch., Teil B*, 1984, **39**, 778.
9 M. J. Frisch, G. W. Trucks, H. B. Schlegel, P. M. W. Gill, B. G. Johnson, M. A. Robb, J. R. Cheeseman, T. Keith, G. A. Petersson, J. A. Montgomery, K. Raghavachari, M. A. Al-Laham, V. G. Zakrzewski, J. V. Ortiz, J. B. Foresman, J. Cioslowski, B. B. Stefanov, A. Nanayakkara, M. Challacombe, C. Y. Peng, P. Y. Ayala, W. Chen, M. W. Wong, J. L. Andres, E. S. Replogle, R. Gomperts, R. L. Martin, D. J. Fox, J. S. Binkley, D. J. Defrees, J. Baker, J. P. Stewart, M. Head-Gordon, C. Gonzalez and J. A. Pople, GAUSSIAN 94, Revision B.1, Gaussian Inc., Pittsburgh, PA, 1995.
10 A. Schäfer, H. Horn and R. Ahlrichs, *J. Chem. Phys.*, 1992, **97**, 2571.
11 A. Schäfer, C. Huber and R. Ahlrichs, *J. Chem. Phys.*, 1994, **100**, 5829.
12 S. Böcker and M. Häser, *Z. Anorg. Allg. Chem.*, 1995, **621**, 258.
13 R. C. Binning, jun. and L. A. Curtiss, *J. Comput. Chem.*, 1990, **11**, 1206.
14 D. B. Chesnut and B. E. Rusiloski, *Chem. Phys.*, 1991, **157**, 105.
15 M. Bühl, W. Thiel, U. Fleischer and W. Kutzelnigg, *J. Phys. Chem.*, 1995, **99**, 4000.
16 W. R. Wadt and P. J. Hay, *J. Chem. Phys.*, 1985, **82**, 284.
17 B. W. Tattershall and E. L. Sandham, *Z. Anorg. Allg. Chem.*, 1996, **622**, 1635.
18 R. Blachnik, K. Hackmann and B. W. Tattershall, *Polyhedron*, 1996, **15**, 1415.
19 R. Blachnik, P. Lönnecke, K. Boldt and B. Engelen, *Acta Crystallogr., Sect. C*, 1994, **50**, 659.
20 E. Fluck, N. Yutronic S. and W. Haubold, *Z. Anorg. Allg. Chem.*, 1976, **420**, 247.
21 B. W. Tattershall and E. L. Sandham, unpublished work.
22 H.-P. Baldus, R. Blachnik, P. Loennecke and B. W. Tattershall, *J. Chem. Soc., Dalton Trans.*, 1991, 2643.
23 B. W. Tattershall, J. Lutz and R. Blachnik, unpublished work.
24 A. R. Quirt, J. S. Martin and K. M. Worvill, NUMARIT, Version 771, SERC NMR Program Library, Daresbury, 1977.
25 G. M. Sheldrick, *SHELXTL Users' Manual*, Version 5, Siemens Analytical X-Ray Instruments, Madison, WI, 1994.

Received 17*th June* 1996; *Paper* 6/04230I